Electronic Supplementary Information for

Temperature-induced single-crystal-to-single-crystal transformation of a binuclear Mn(II) complex into a 1D chain polymer

Peng Jiang, Fen Peng and Yanmei Chen*
Hubei Key Laboratory for Processing and Application of Catalytic Materials, College of Chemical Engineering, Huanggang Normal University, Huanggang, 438000, China.

Table S1 Selected Bond Lengths (Å) and Bond Angles (°) for **1** and **2**.

Complex **1**			
Mn(1)-O(1)	2.1360(12)	Mn(1)-O(2)	2.1902(13)
Mn(1)-O(3)	2.1720(12)	Mn(1)-O(4)	2.2048(11)
Mn(1)-O(4)A	2.2101(12)	Mn(1)-O(5)	2.2220(12)
O(1)-Mn(1)-O(3)	168.07(5)	O(1)-Mn(1)-O(2)	74.93(4)
O(3)-Mn(1)-O(2)	93.26(5)	O(1)-Mn(1)-O(4)	108.11(5)
O(3)-Mn(1)-O(4)	74.50(4)	O(2)-Mn(1)-O(4)	97.13(5)
O(1)-Mn(1)-O(4)A	93.77(4)	O(3)-Mn(1)-O(4)A	98.13(4)
O(2)-Mn(1)-O(4)A	168.06(4)	O(4)-Mn(1)-O(4)A	82.55(5)
O(1)-Mn(1)-O(5)	89.47(5)	O(3)-Mn(1)-O(5)	89.57(4)
O(2)-Mn(1)-O(5)	93.26(5)	O(4)-Mn(1)-O(5)	161.39(4)
O(4)A-Mn(1)-O(5)	90.43(5)	C(7)-O(1)-Mn(1))	115.71(10)
C(14)-O(3)-Mn(1)	114.78(10)	N(1)-O(4)-Mn(1)	109.04(8)
N(1)-O(4)-Mn(1)A	107.65(8)	Mn(1)-O(4)-Mn(1)A	97.45(5)
Mn(1)-O(5)-H(5A)	110.7	Mn(1)-O(5)-H(5B)	119.1
N(3)-O(2)-Mn(1)	109.05(9)		

Symmetry transformations used to generate equivalent atoms: A: -x+1,-y+1,-z

Complex **2**			
Mn(1)-O(1)A	2.1251(13)	Mn(1)-O(1)	2.1251(13)
Mn(1)-O(2)B	2.2135(17)	Mn(1)-O(2)C	2.2135(17)
Mn(1)-O(2)A	2.2518(17)	Mn(1)-O(2)	2.2518(17)
O(2)-Mn(1)D	2.2135(17)	O(1)A-Mn(1)-O(1)	177.20(14)
O(1)A-Mn(1)-O(2)B	96.21(8)	O(1)-Mn(1)-O(2)B	85.90(6)
O(1)A-Mn(1)-O(2)C	85.90(6)	O(1)-Mn(1)-O(2)C	96.21(8)
O(2)B-Mn(1)-O(2)C	82.78(8)	O(1)A-Mn(1)-O(2)A	73.63(6)
O(1)-Mn(1)-O(2)A	104.17(8)	O(2)B-Mn(1)-O(2)A	101.81(5)
O(2)C-Mn(1)-O(2)A	159.34(6)	O(1)A-Mn(1)-O(2)	104.17(8)
O(1)-Mn(1)-O(2)	73.62(6)	O(2)B-Mn(1)-O(2)	159.34(6)
O(2)C-Mn(1)-O(2)	101.81(5)	O(2)A-Mn(1)-O(2)	81.07(8)
N(1)-O(2)-Mn(1)D	114.22(12)	N(1)-O(2)-Mn(1)	108.13(12)
Mn(1)D-O(2)-Mn(1)	98.08(5)	C(7)-O(1)-Mn(1)	117.62(13)

Symmetry transformations used to generate equivalent atoms:

A: -x,-y+1,z; B: -x+0,y+0,z-1/2; C: x+0,-y+1,z-1/2; D: x+0,-y+1,z+1/2.

Table S2 Hydrogen Bond Lengths (Å) and Bond Angles (°) for **1.**

D-H···A	d(D-H)	d(H···A)	d(D···A)	<(DHA)
N(1)-H(1)···N(2)B	0.85	2.22	3.039(2)	161.0
N(2)-H(2A)···O(5)C	0.81	2.39	3.132(2)	152.8
N(2)-H(2B)···O(6)D	0.83	2.18	3.006(3)	171.0
O(5)-H(5A)···O(3)E	0.85	2.00	2.8049(18)	158.2
O(5)-H(5B)···O(2)E	0.85	1.86	2.6755(17)	159.9
O(6)-H(6B)···O(2)	0.85	2.09	2.769(2)	136.5
N(4)-H(4A)···O(4)F	0.81	2.25	3.057(2)	177.3
N(4)-H(4B)···O(6)G	0.81	2.35	3.055(3)	145.4

Symmetry transformations used to generate equivalent atoms:

A: -x+1,-y+1,-z; B: -x+3/2,y-1/2,-z-1/2; C: x+1/2,-y+3/2,z-1/2;

D: x-1/2,-y+3/2,z-1/2; E: -x+1,-y+2,-z; F: -x+3/2,y+1/2,-z+1/2

G: x-1/2,-y+3/2,z+1/2.

Table S3 Hydrogen Bond Lengths (Å) and Bond Angles (°) for **2**

D-H···A	d(D-H)	d(H···A)	d(D···A)	<(DHA)
N(2)-H(2C)···O(2)E	0.95	2.01	2.964(2)	176.0
N(2)-H(2C)···N(1)E	0.95	2.44	3.267(2)	144.7
C(2)-H(2A)···O(1)	0.93	2.47	2.787(2)	99.8

Symmetry transformations used to generate equivalent atoms:

A: -x,-y+1,z; B: -x+0,y+0,z-1/2; C: x+0,-y+1,z-1/2;

D: x+0,-y+1,z+1/2; E: -x+1/2,y-1/2,z.

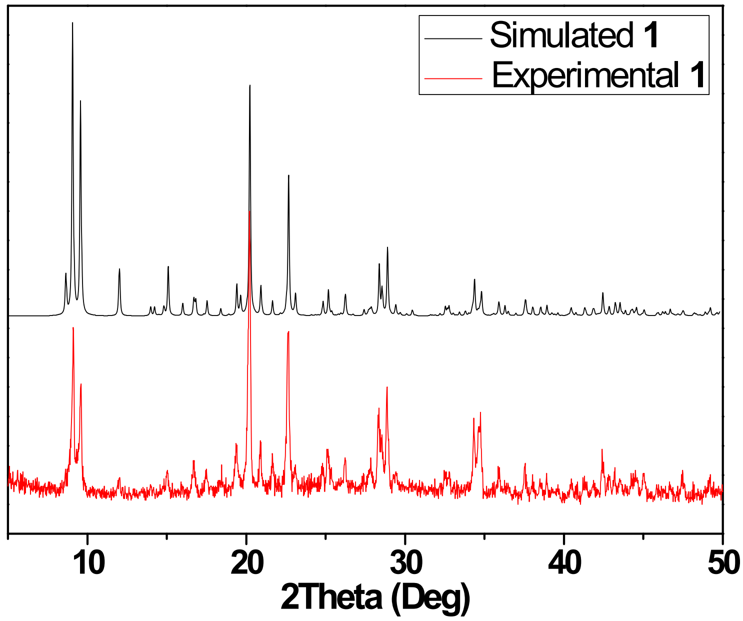

Fig S1 The powder XRD spectra of **1.**

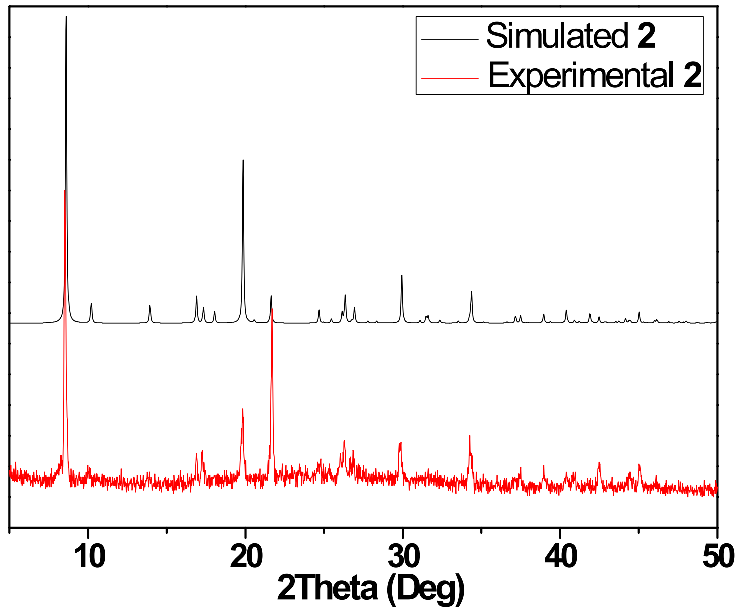

Fig S2 The powder XRD spectra of **2.**

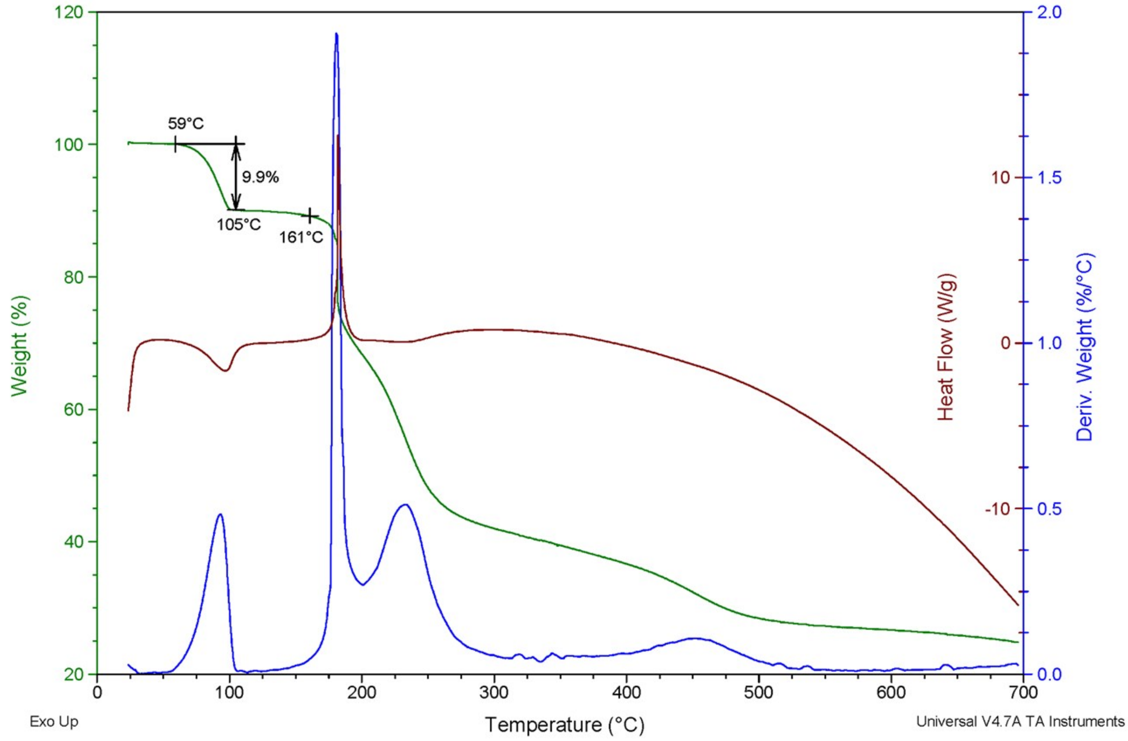

Fig S3 The TGA-DSC curve of complex **1**.

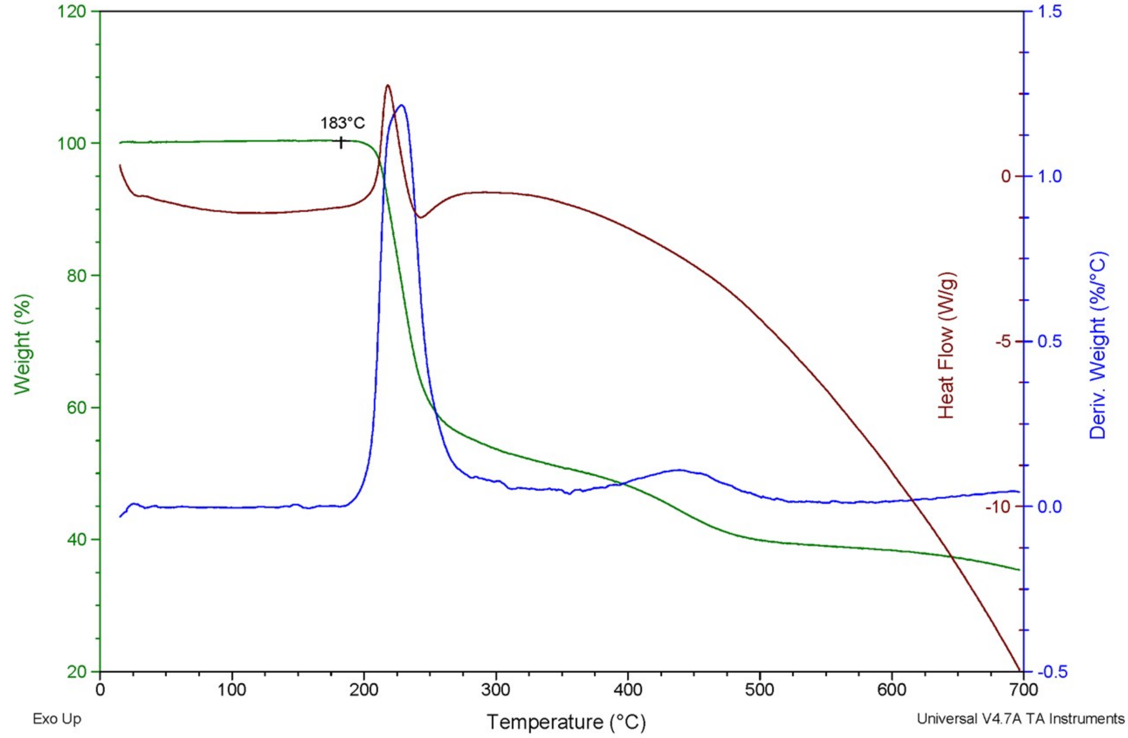

Fig S4 The TGA-DSC curve of complex **2**.

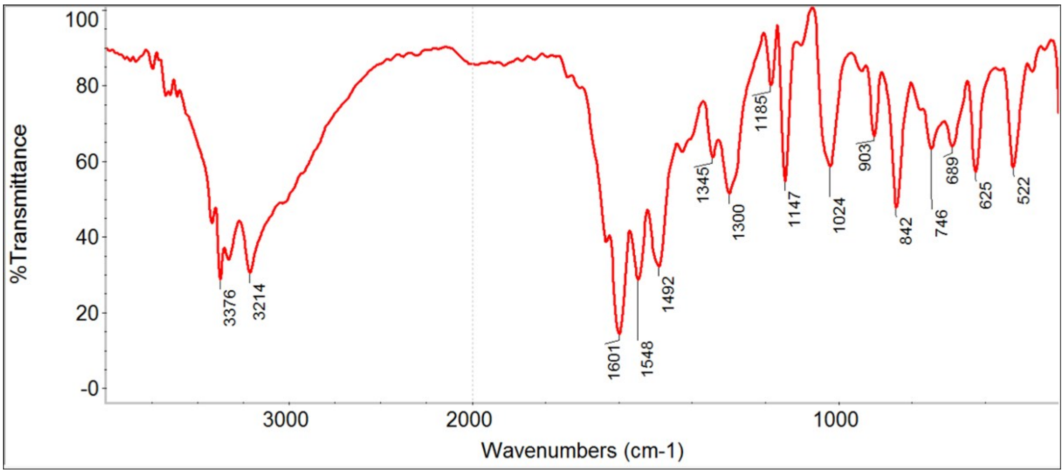

Fig S5 The IR spectrum of complex **1**

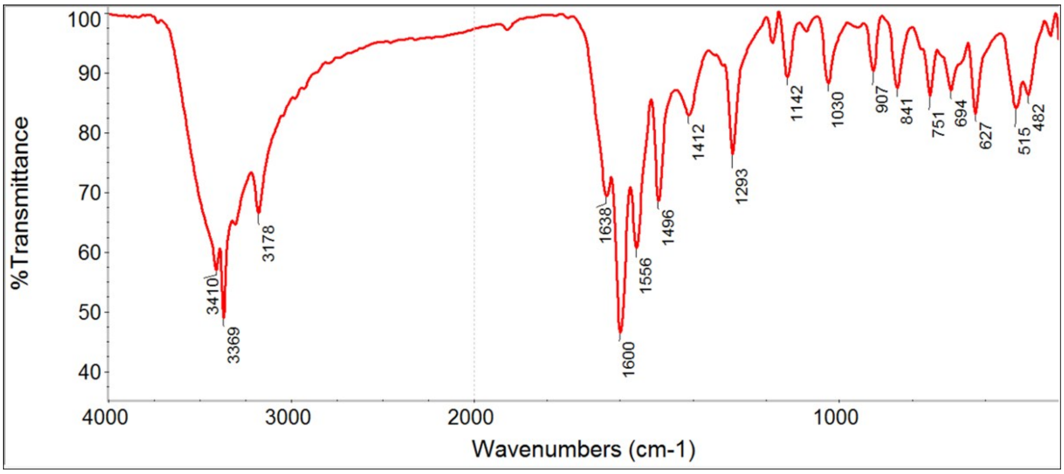

Fig S6 The IR spectrum of complex **2**

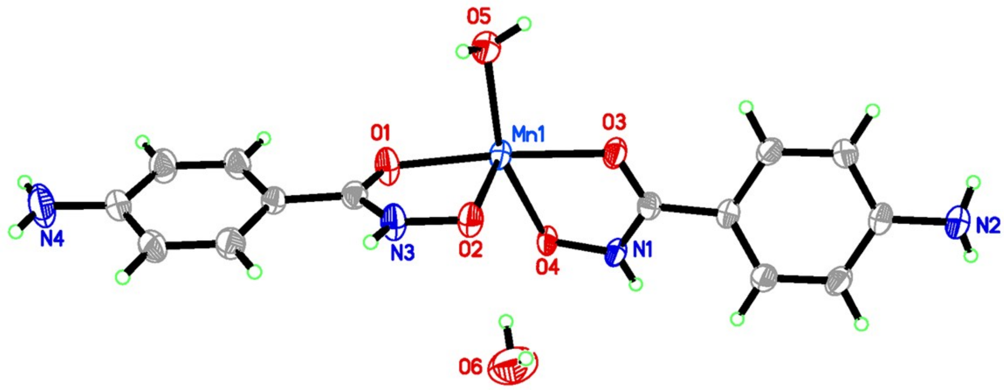

Fig S7 ORTEP figure of asymmetric units in **1** (with 50% probability).

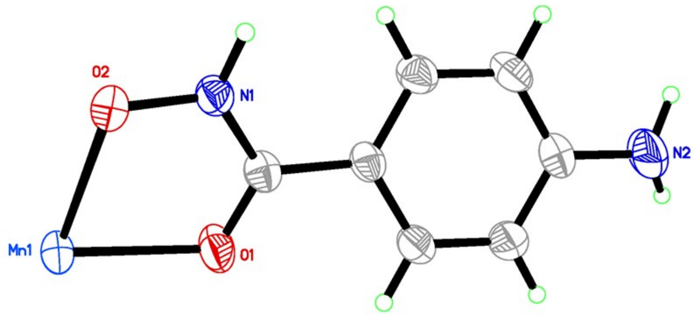

Fig S8 ORTEP figure of asymmetric units in **2** (with 50% probability).

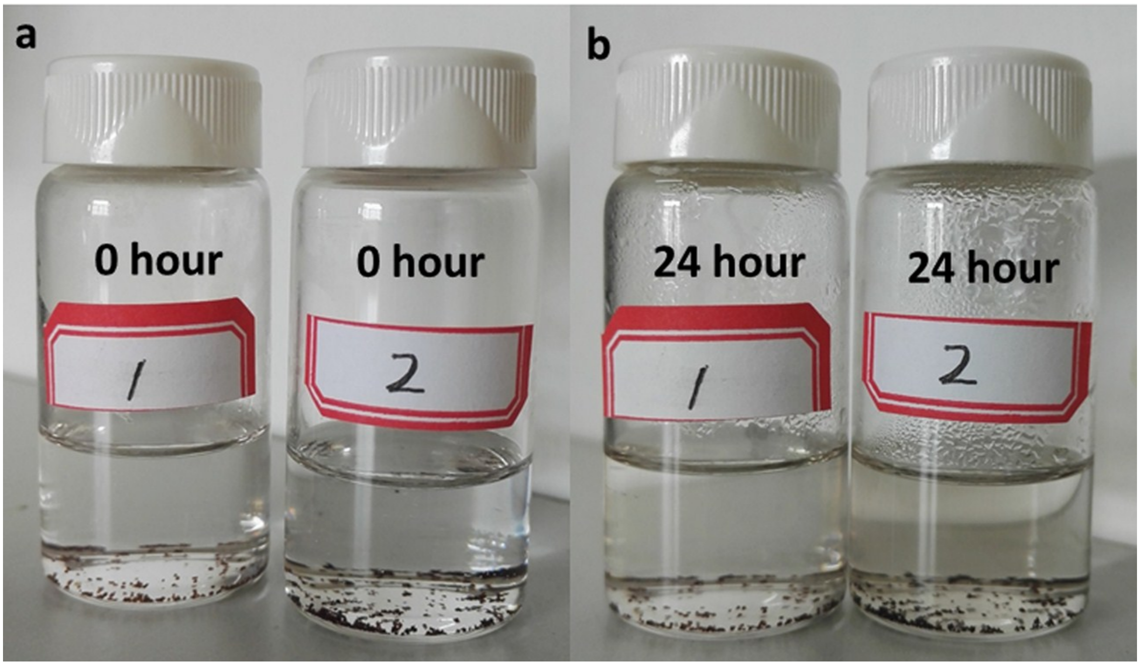

Fig S9 24-hours moisture absorption experiments of complexes **1** and **2**.

The crystals are placed in a bottle with water for 24 hours; the results of the crystals do not change, indicating that the crystals do not absorb moisture (Fig S9).

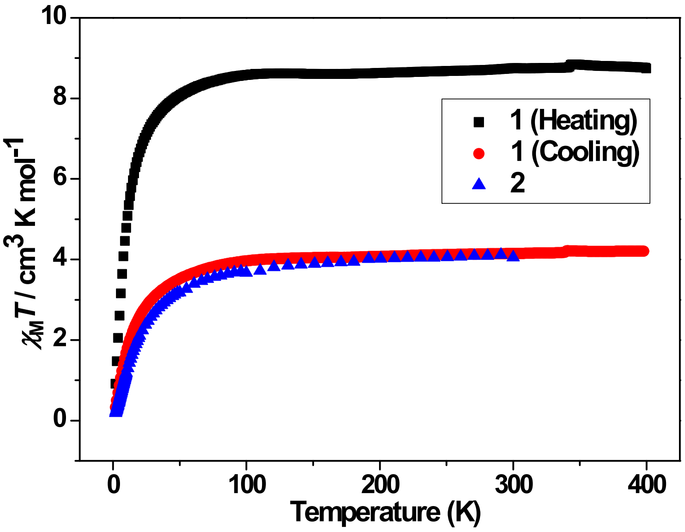

Fig S10 Temperature dependence of magnetic susceptibilities in the form of $\chi_M T$ vs T for **1** at 1 kOe (heating-cooling cycle from 1.8-400 K), and $\chi_M T$ vs T for **2** (2-300K).

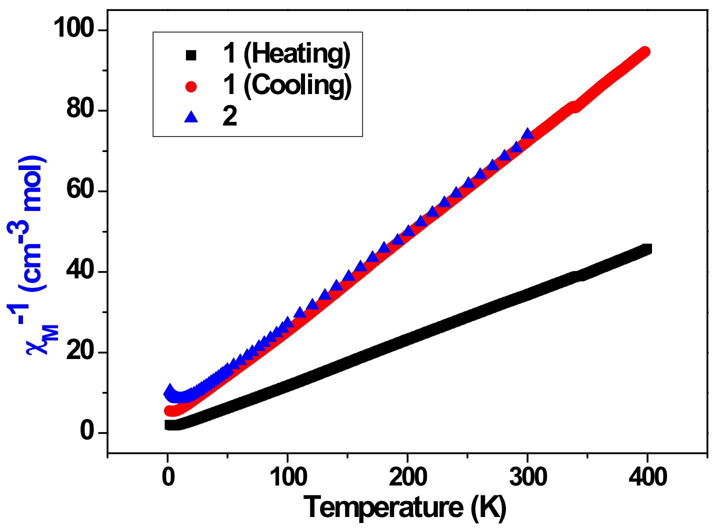

Fig S11 Temperature dependence of magnetic susceptibilities in the form of χ_M^{-1} *vs* T for **1** at 1 kOe (heating-cooling cycle from 1.8-400 K), and χ_M^{-1} vs T for **2** (2-300K).

Heating-cooling cycle magnetic properties discussion

Heating-cooling cycle of magnetic susceptibilities data were recorded for polycrystalline samples of **1** at an applied magnetic field of 1000 Oe in the temperature range of 1.8-400 K. As seen in Fig. S10, The $\chi_M T$ increases steeply from 0.95 cm^3 K mol^{-1} to 8.38 cm^3 K mol^{-1} from 1.8 K to 70 K and then at higher temperature increases more gradually to reach 8.75 cm^3 K mol^{-1} at 400 K. When heated to 400 K, complex **1** has been transformed into complex **2**. The $\chi_M T$ curve of **1** (cooling) is very close to the $\chi_M T$ curve of **2**. The Curie-Weiss curve of **1** (cooling) is very close to **2**, too (Fig. S11). The result is also proved that complex **1** can be converted to compound 2 by dehydration at high temperature.